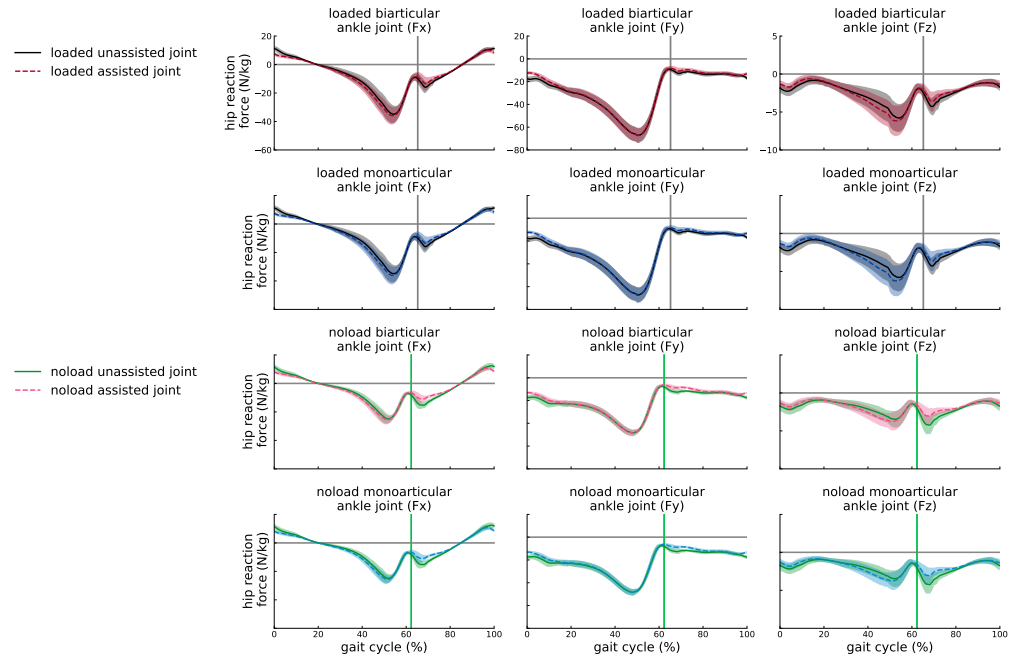
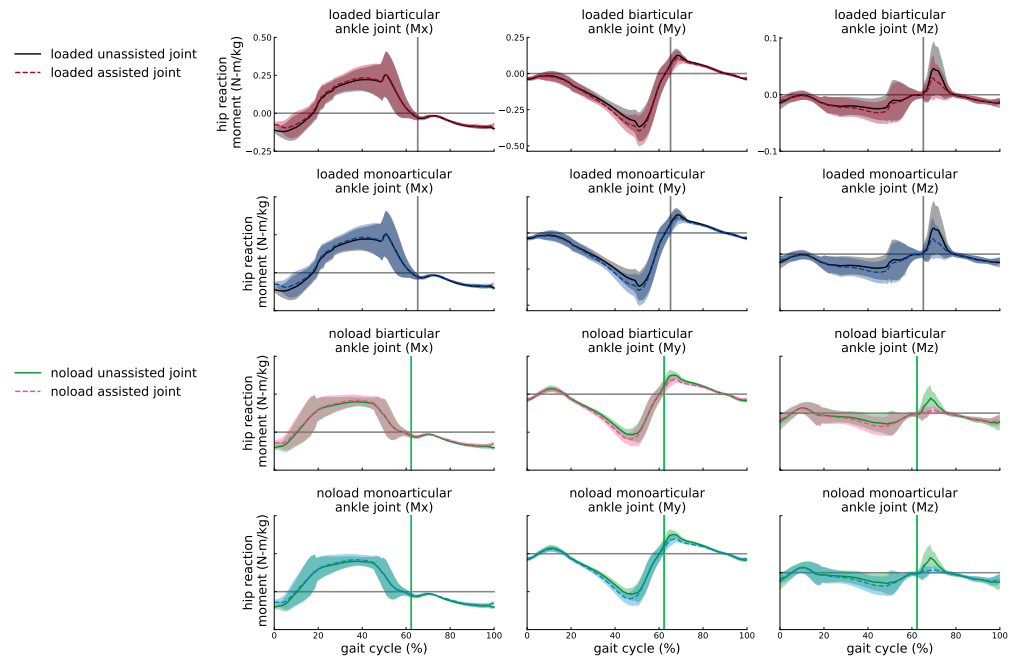


## Supporting Document for Joint Reaction Forces and Moments



**Fig B1. Ideal devices effect on joint reaction forces of the ankle joint.** The reaction forces of the ankle joint in anterior-Posterior ( $F_x$ ), compressive ( $F_y$ ), and medial-lateral ( $F_z$ ) directions. The blue and red shades represent the reaction forces of subjects assisted by ideal monoarticular and biarticular exoskeletons, respectively. The black and green profiles represent the reaction forces of unassisted subjects in *loaded* and *noload* conditions, respectively. The curves are averaged over 7 subjects with 3 trials and normalized by subject mass; shaded regions around the mean profile indicate standard deviation of the profile.



**Fig B2. Ideal devices effect on joint reaction moments of the ankle joint.** The reaction moments of the ankle joint in adduction-abduction ( $M_x$ ), internal-external rotation ( $M_y$ ), and medial-lateral ( $M_z$ ) directions. The blue and red shades represent the reaction moments of subjects assisted by ideal monoarticular and biarticular exoskeletons, respectively. The black and green profiles represent the reaction forces of unassisted subjects in *loaded* and *noload* conditions, respectively. The curves are averaged over 7 subjects with 3 trials and normalized by subject mass; shaded regions around the mean profile indicate standard deviation of the profile.

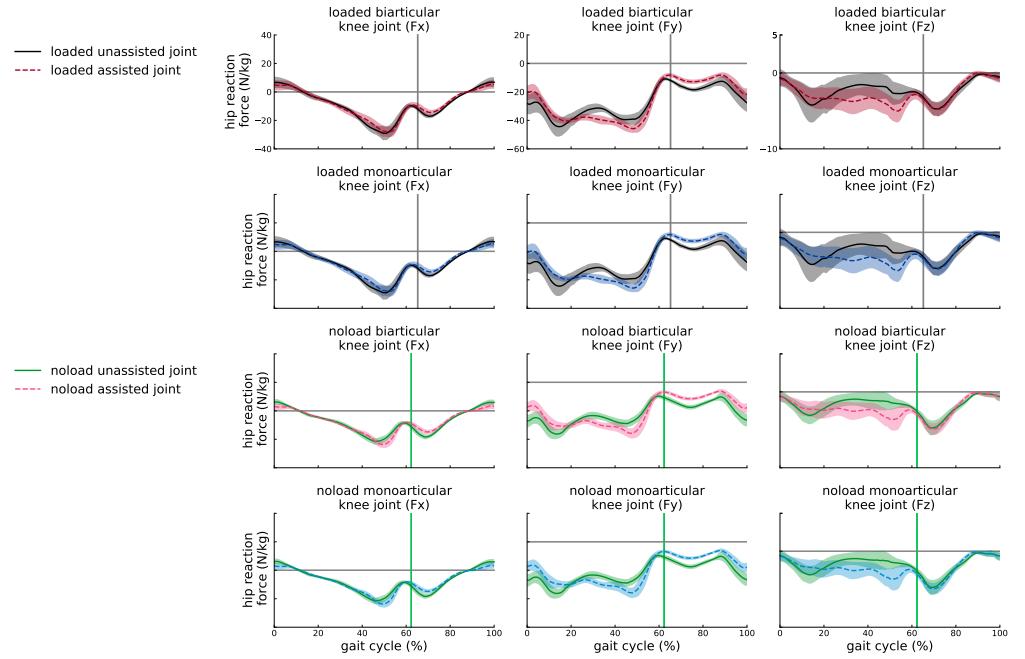


**Fig B3. Ideal devices effect on joint reaction forces of the knee joint.** The reaction forces of the knee joint in anterior-Posterior ( $F_x$ ), compressive ( $F_y$ , i.e., tibofemoral force), and medial-lateral ( $F_z$ ) directions. The blue and red shades represent the reaction forces of subjects assisted by ideal monoarticular and biarticular exoskeletons, respectively. The black and green profiles represent the reaction forces of unassisted subjects in *loaded* and *noload* conditions, respectively. The curves are averaged over 7 subjects with 3 trials and normalized by subject mass; shaded regions around the mean profile indicate standard deviation of the profile.

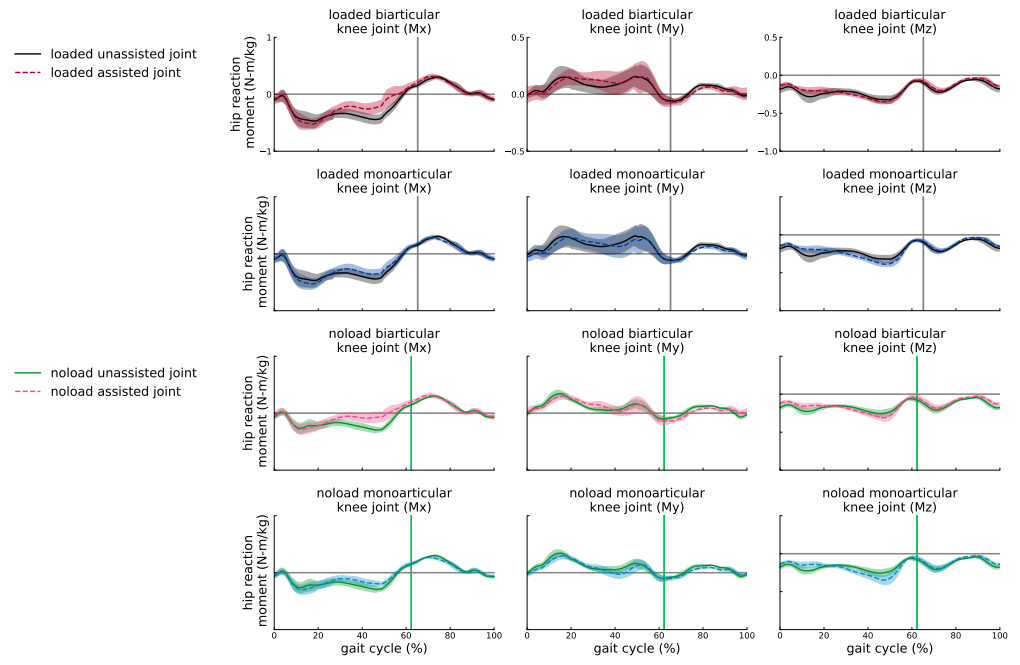


**Fig B4. Ideal devices effect on joint reaction moments of the knee joint.** The reaction moments of the knee joint in adduction-abduction ( $M_x$ ), internal-external rotation ( $M_y$ ), and medial-lateral ( $M_z$ ) directions. The blue and red shades represent the reaction moments of subjects assisted by ideal monoarticular and biarticular exoskeletons, respectively. The black and green profiles represent the reaction forces of unassisted subjects in *loaded* and *noload* conditions, respectively. The curves are averaged over 7 subjects with 3 trials and normalized by subject mass; shaded regions around the mean profile indicate standard deviation of the profile.

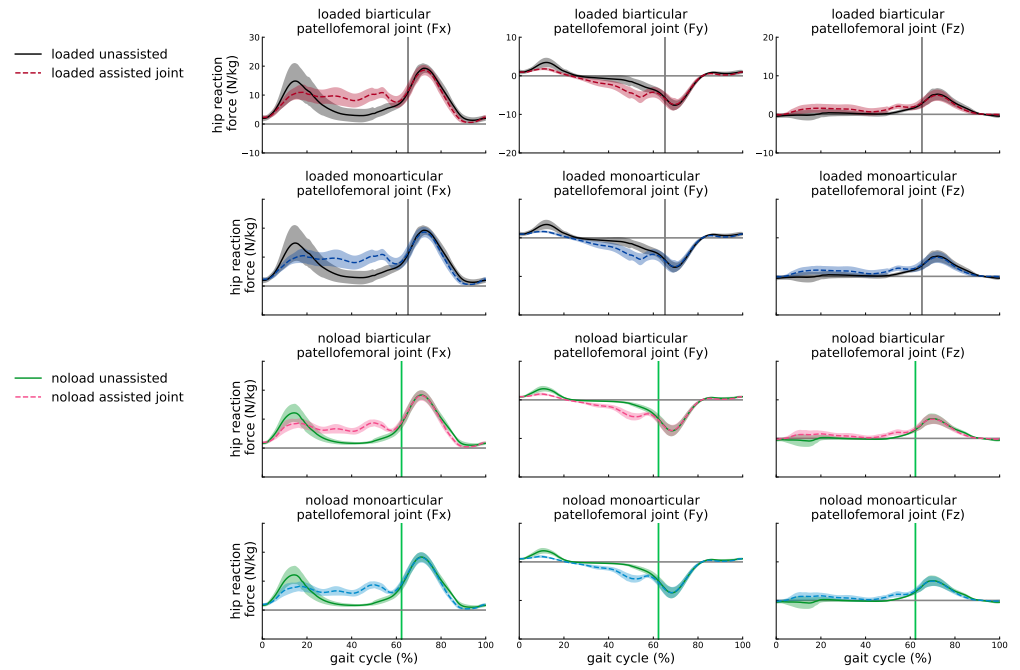


**Fig B5. Ideal devices effect on joint reaction forces of the patellofemoral joint.**  
The reaction forces of the patellofemoral joint in anterior-Posterior ( $F_x$ ), compressive ( $F_y$ ), and medial-lateral ( $F_z$ ) directions. The blue and red shades represent the reaction forces of subjects assisted by ideal monoarticular and biarticular exoskeletons, respectively. The black and green profiles represent the reaction forces of unassisted subjects in *loaded* and *noload* conditions, respectively. The curves are averaged over 7 subjects with 3 trials and normalized by subject mass; shaded regions around the mean profile indicate standard deviation of the profile.

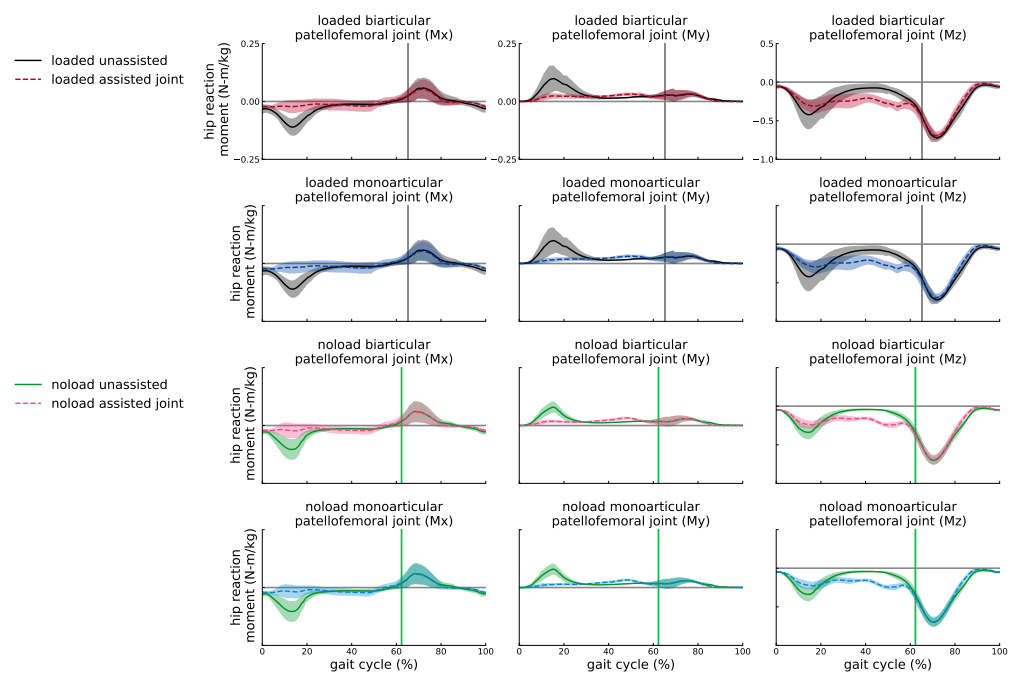


**Fig B6. Ideal devices effect on joint reaction moments of the patellofemoral joint.** The reaction moments of the patellofemoral joint in adduction-abduction ( $M_x$ ), internal-external rotation ( $M_y$ ), and medial-lateral ( $M_z$ ) directions. The blue and red shades represent the reaction moments of subjects assisted by ideal monoarticular and biarticular exoskeletons, respectively. The black and green profiles represent the reaction forces of unassisted subjects in *loaded* and *noload* conditions, respectively. The curves are averaged over 7 subjects with 3 trials and normalized by subject mass; shaded regions around the mean profile indicate standard deviation of the profile.

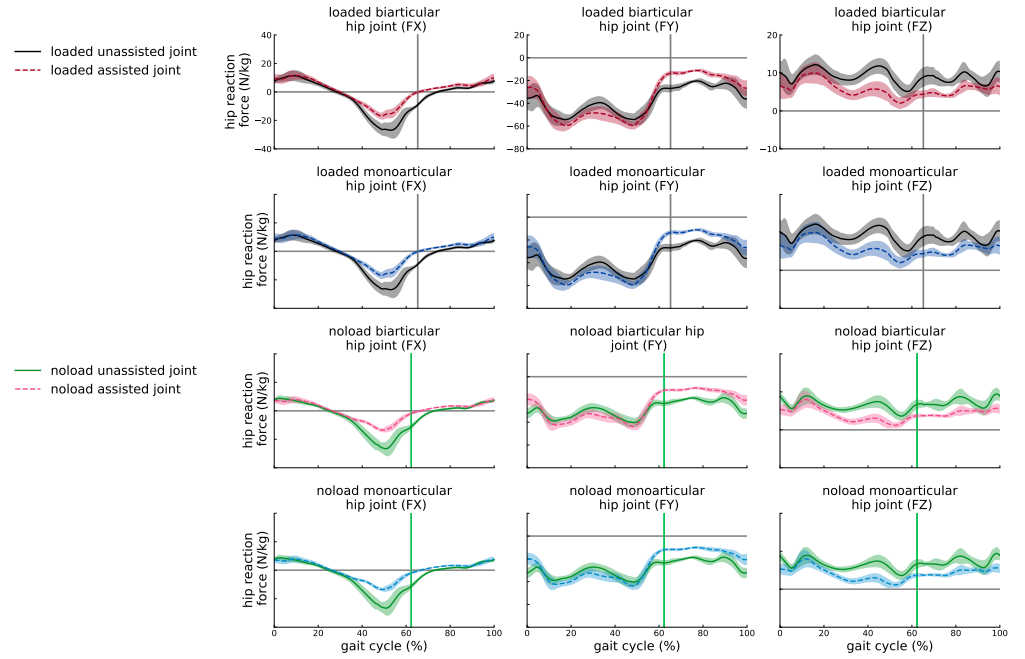


**Fig B7. Ideal devices effect on joint reaction forces of the hip joint.** The reaction forces of the hip joint in anterior-Posterior ( $F_x$ ), compressive ( $F_y$ ), and medial-lateral ( $F_z$ ) directions. The blue and red shades represent the reaction forces of subjects assisted by ideal monoarticular and biarticular exoskeletons, respectively. The black and green profiles represent the reaction forces of unassisted subjects in *loaded* and *noload* conditions, respectively. The curves are averaged over 7 subjects with 3 trials and normalized by subject mass; shaded regions around the mean profile indicate standard deviation of the profile.

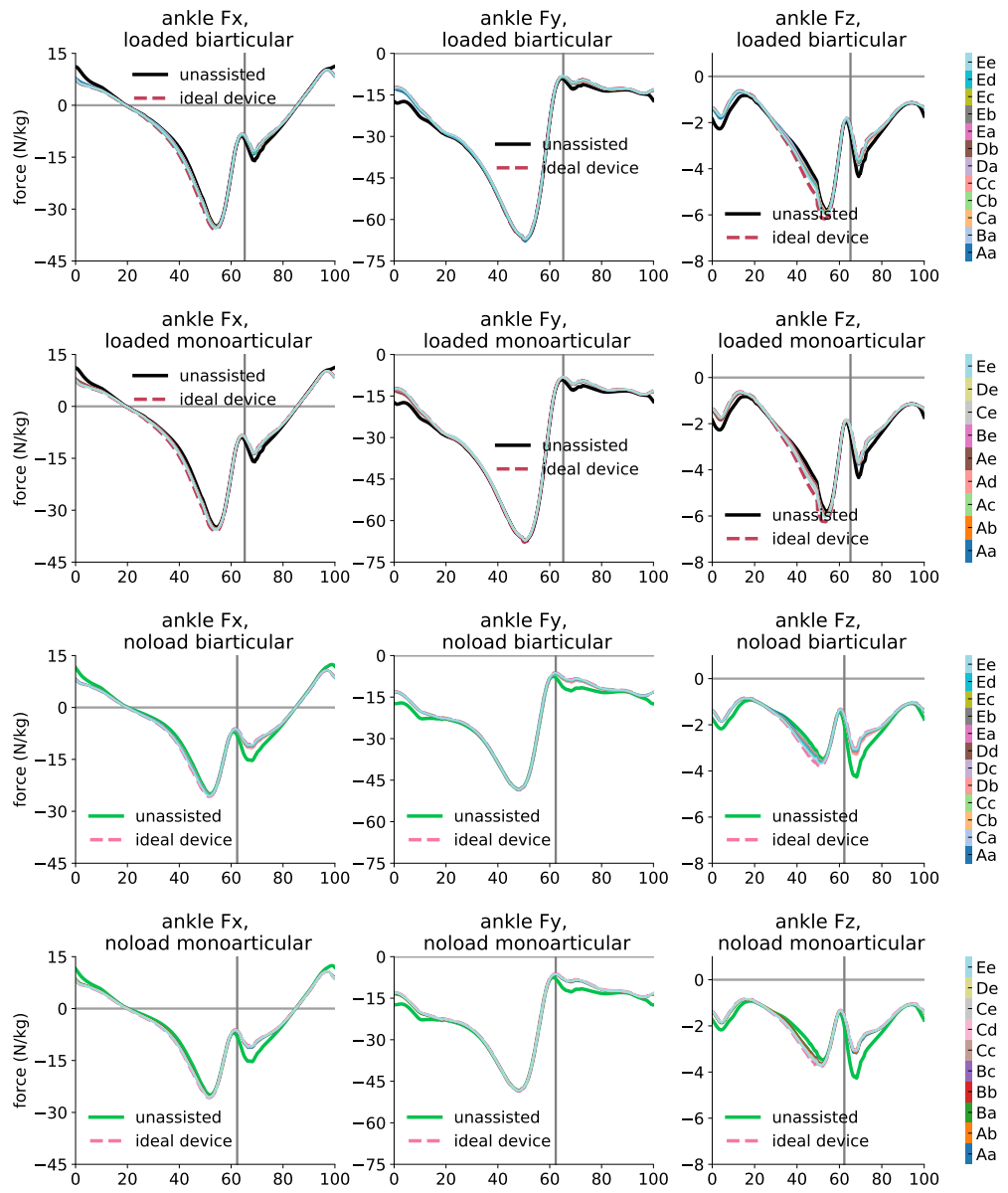


**Fig B8. Optimal devices effect on joint reaction forces of the ankle joint.** The reaction forces of the ankle joint in anterior-Posterior ( $F_x$ ), compressive ( $F_y$ ), and medial-lateral ( $F_z$ ) directions. The color bars represent the reaction forces of subjects assisted by constrained optimal exoskeletons. The black and green profiles represent the reaction forces of unassisted subjects in *loaded* and *noload* conditions, respectively. The curves are averaged over 7 subjects with 3 trials and normalized by subject mass.

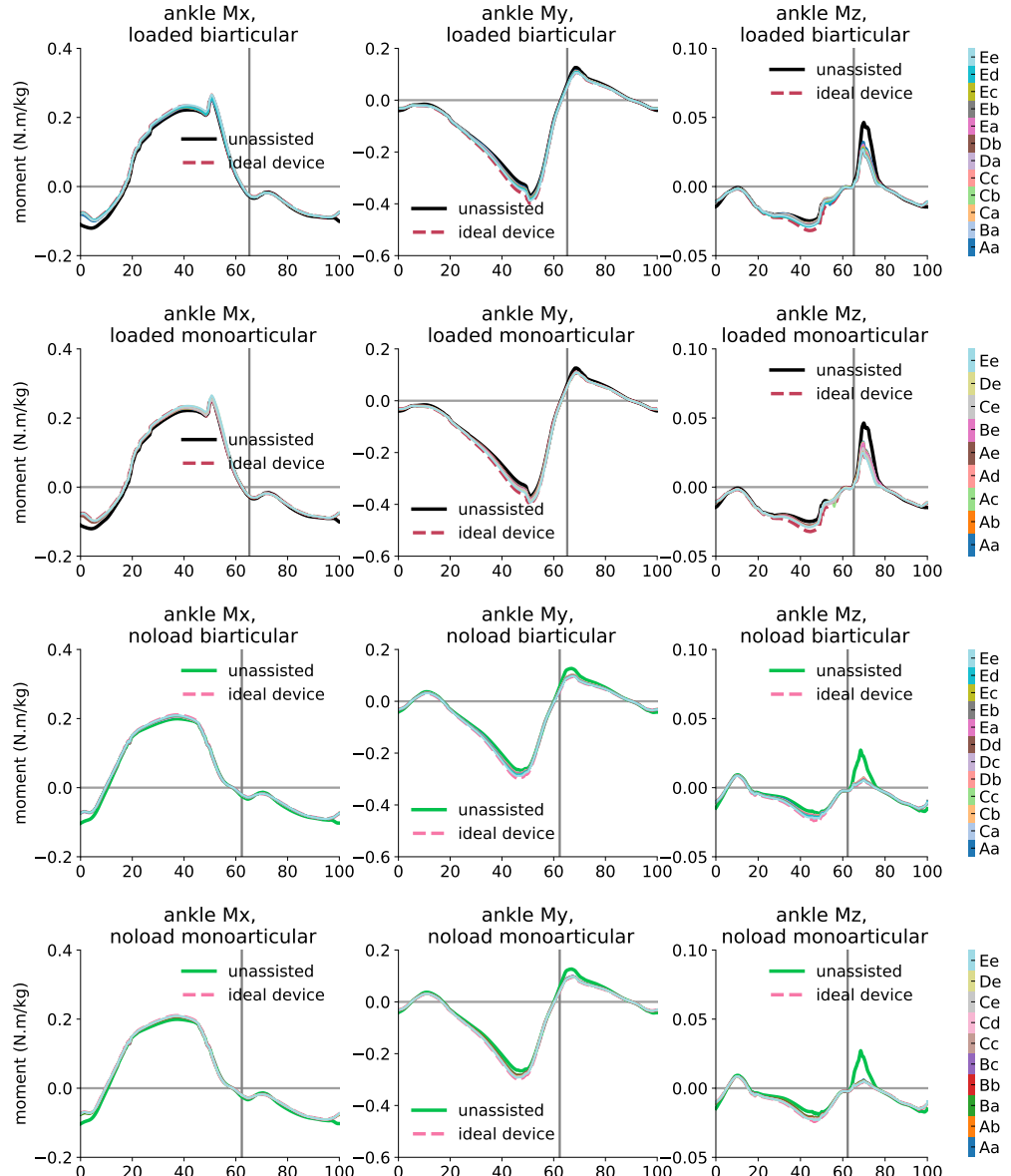


**Fig B9. Optimal devices effect on joint reaction moments of the ankle joint.** The reaction moments of the ankle joint in adduction-abduction ( $M_x$ ), internal-external rotation ( $M_y$ ), and medial-lateral ( $M_z$ ) directions. The color bars represent the reaction moments of subjects assisted by constrained optimal exoskeletons. The black and green profiles represent the reaction forces of unassisted subjects in *loaded* and *noload* conditions, respectively. The curves are averaged over 7 subjects with 3 trials and normalized by subject mass.

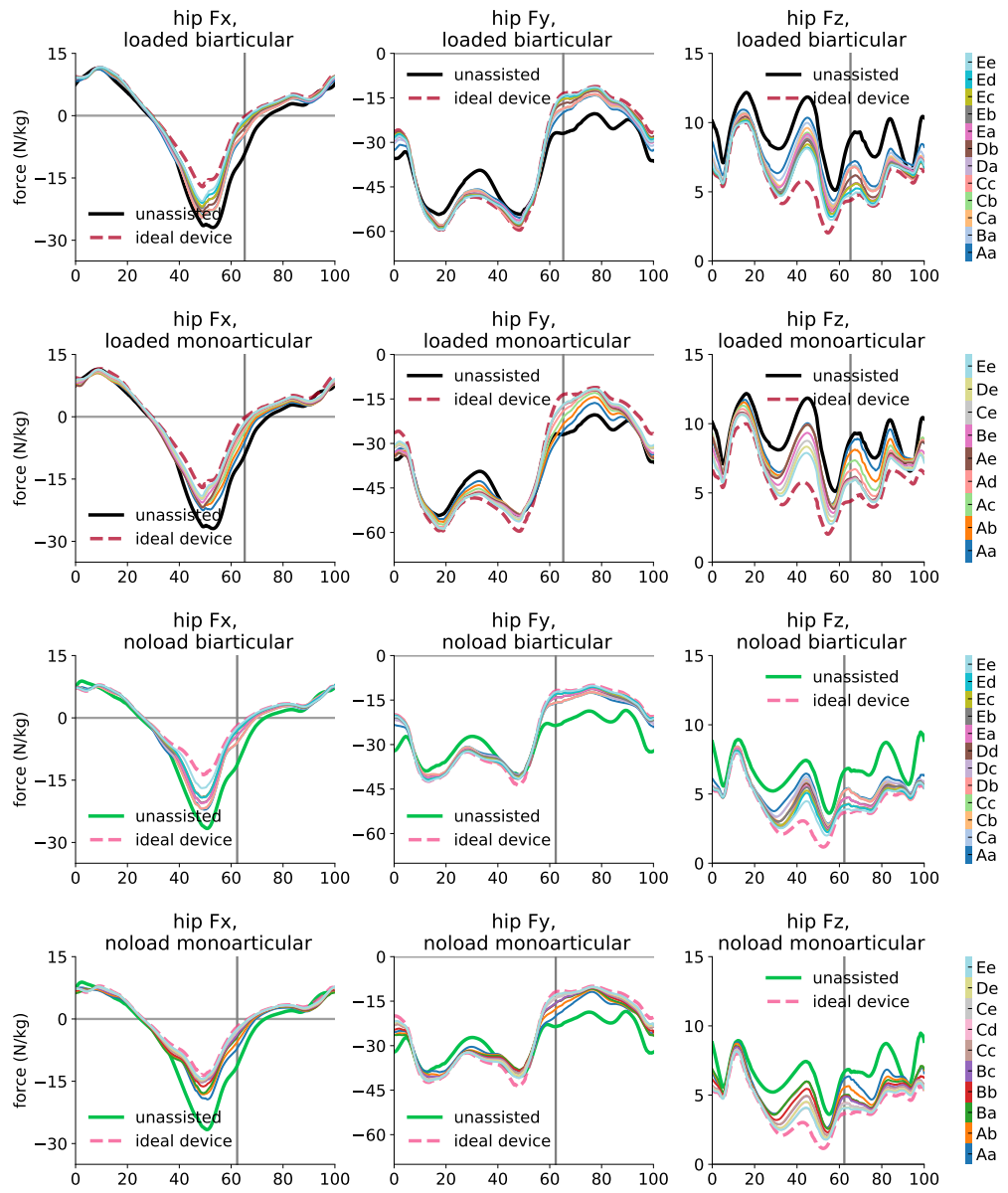


**Fig B10. Optimal devices effect on joint reaction forces of the hip joint.** The reaction forces of the hip joint in anterior-Posterior ( $F_x$ ), compressive ( $F_y$ ), and medial-lateral ( $F_z$ ) directions. The color bars represent the reaction forces of subjects assisted by constrained optimal exoskeletons. The black and green profiles represent the reaction forces of unassisted subjects in *loaded* and *noload* conditions, respectively. The curves are averaged over 7 subjects with 3 trials and normalized by subject mass.

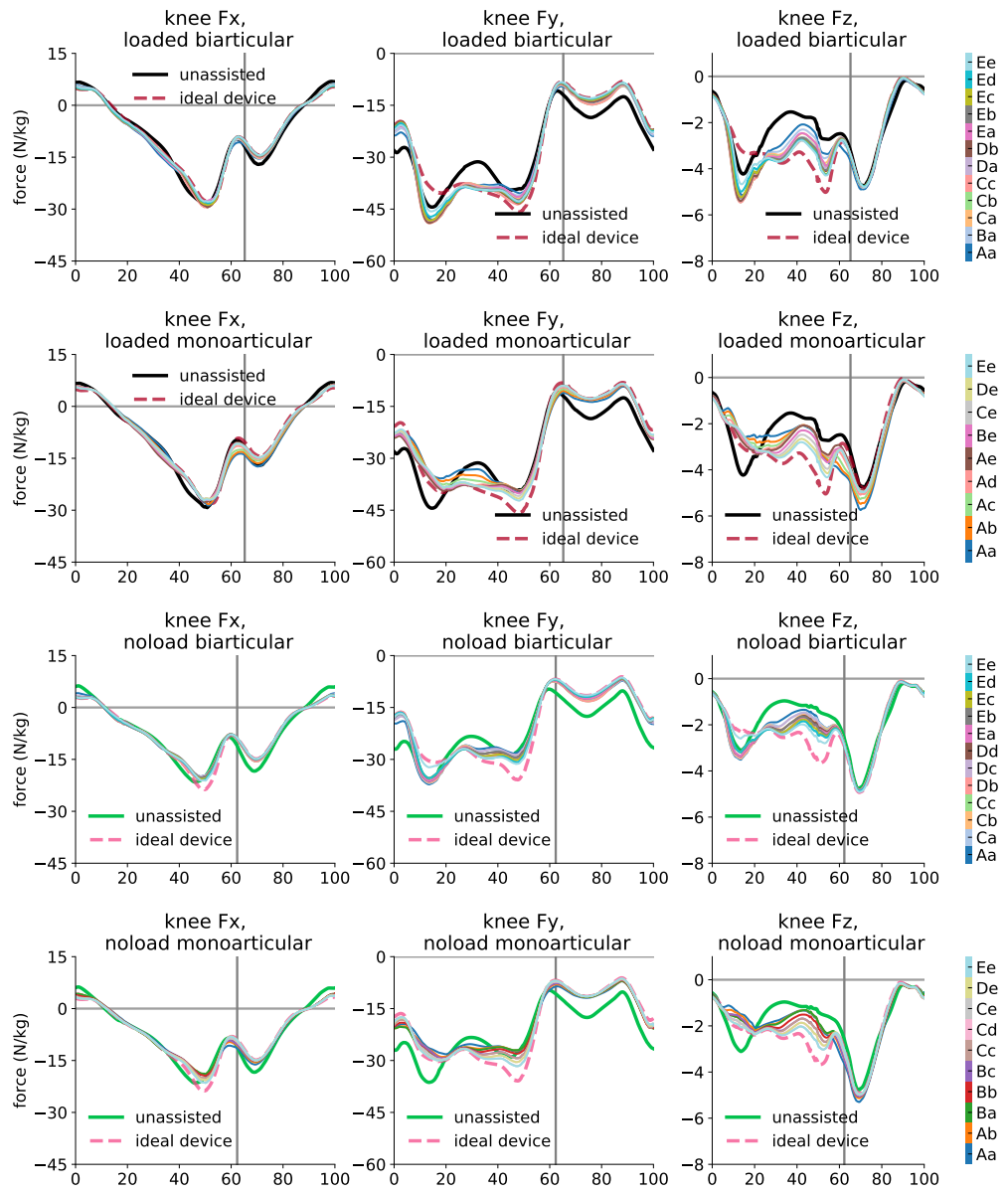


**Fig B11. Optimal devices effect on joint reaction forces of the knee joint.** The reaction forces of the knee joint in anterior-Posterior ( $F_x$ ), compressive ( $F_y$ ), and medial-lateral ( $F_z$ ) directions. The color bars represent the reaction forces of subjects assisted by constrained optimal exoskeletons. The black and green profiles represent the reaction forces of unassisted subjects in *loaded* and *noload* conditions, respectively. The curves are averaged over 7 subjects with 3 trials and normalized by subject mass.

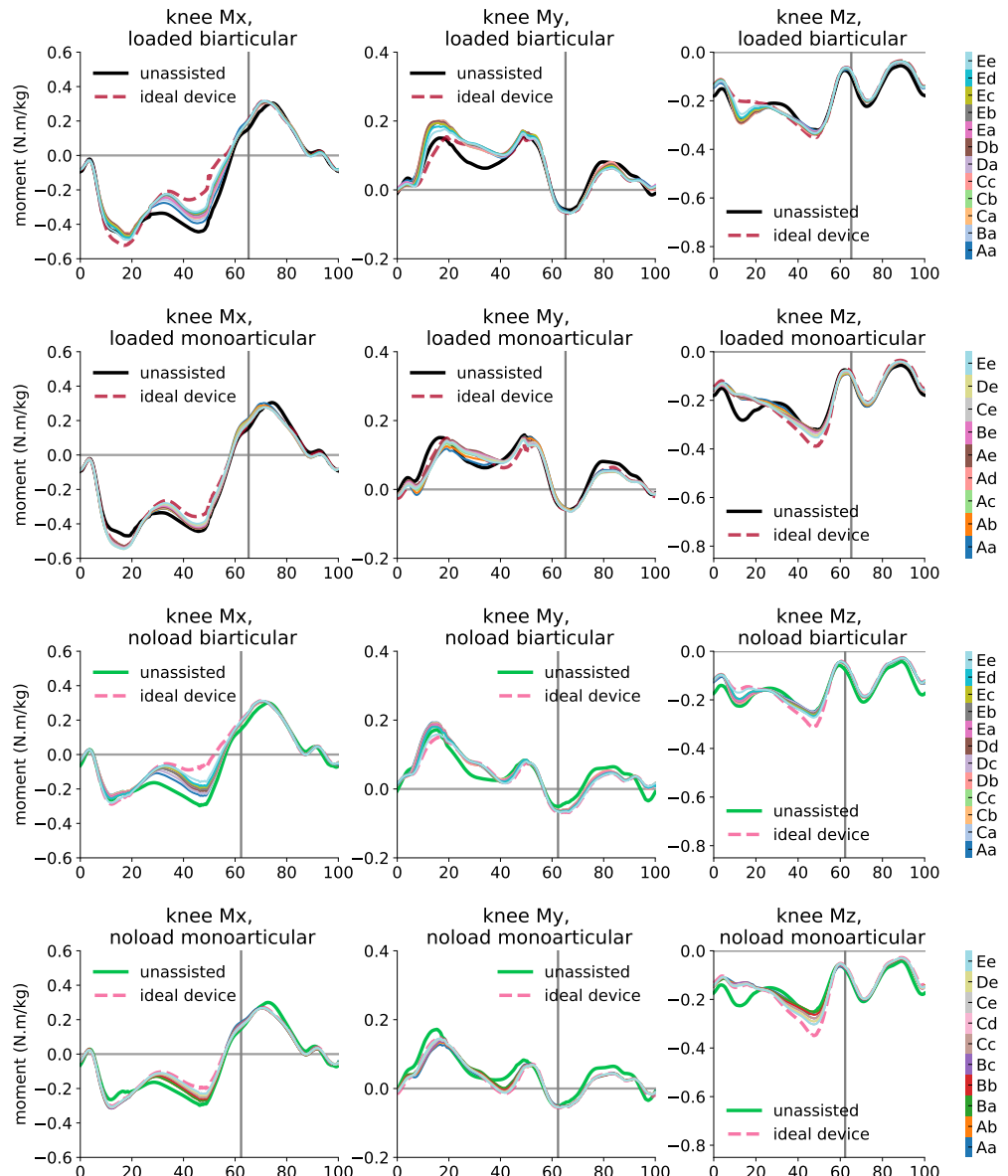


**Fig B12. Optimal devices effect on joint reaction moments of the knee joint.** The reaction moments of the knee joint in adduction-abduction ( $M_x$ ), internal-external rotation ( $M_y$ ), and medial-lateral ( $M_z$ ) directions. The color bars represent the reaction forces of subjects assisted by constrained optimal exoskeletons. The black and green profiles represent the reaction moments of unassisted subjects in *loaded* and *noload* conditions, respectively. The curves are averaged over 7 subjects with 3 trials and normalized by subject mass.

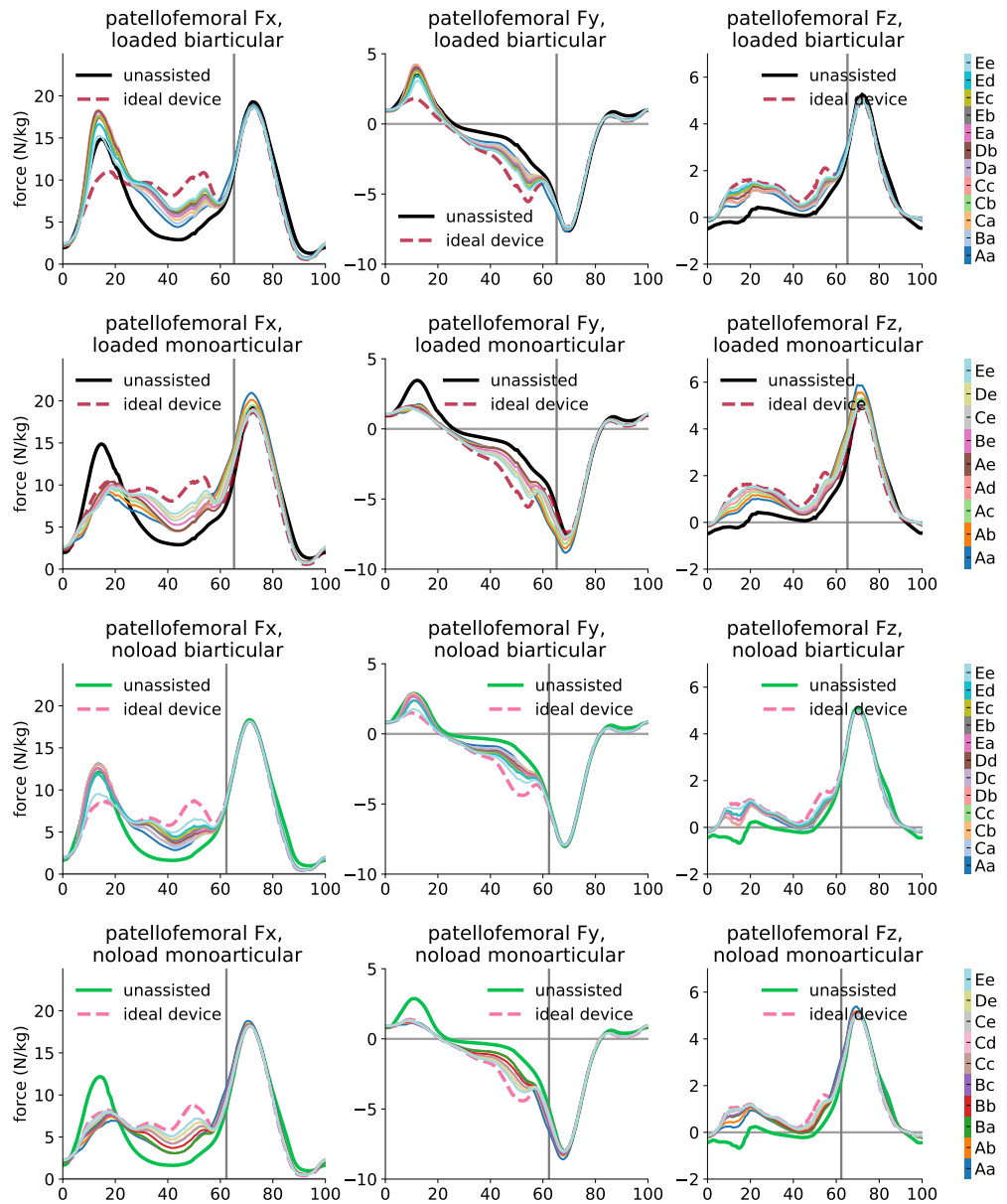


**Fig B13. Optimal devices effect on joint reaction forces of the patellofemoral joint.** The reaction forces of the patellofemoral joint in anterior-Posterior ( $F_x$ ), compressive ( $F_y$ ), and medial-lateral ( $F_z$ ) directions. The color bars represent the reaction forces of subjects assisted by constrained optimal exoskeletons. The black and green profiles represent the reaction forces of unassisted subjects in *loaded* and *noload* conditions, respectively. The curves are averaged over 7 subjects with 3 trials and normalized by subject mass.

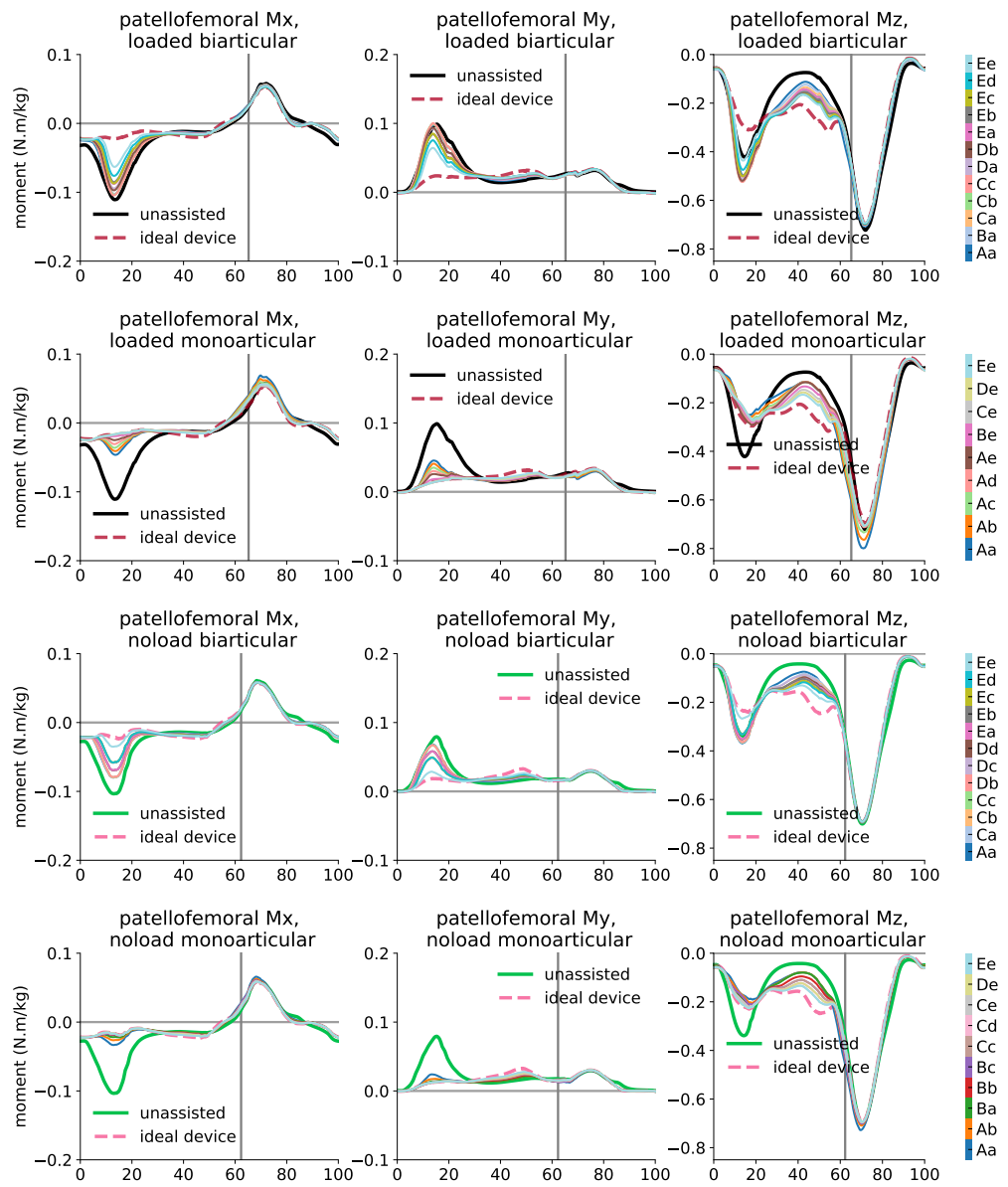


**Fig B14. Optimal devices effect on joint reaction moments of the patellofemoral joint.** The reaction moments of the patellofemoral joint in adduction-abduction ( $M_x$ ), internal-external rotation ( $M_y$ ), and medial-lateral ( $M_z$ ) directions. The color bars represent the reaction moments of subjects assisted by constrained optimal exoskeletons. The black and green profiles represent the reaction forces of unassisted subjects in *loaded* and *noload* conditions, respectively. The curves are averaged over 7 subjects with 3 trials and normalized by subject mass.